

A plasma window for transmission of particle beams and radiation from vacuum to atmosphere for various applications*

Ady Hershcovitch^{†,a)}

Brookhaven National Laboratory, Upton, New York 11973

(Received 17 November 1997; accepted 8 January 1998)

Many industrial and scientific processes like ion material modification, electron beam melting, and welding, as well as generation of synchrotron radiation are performed exclusively in vacuum nowadays, since electron guns, ion guns, their extractors, and accelerators must be kept at a reasonably high vacuum. Consequently, there are numerous limitations, among which are low production rates due to required pumping time, limits on the size of target objects, and degradation of particle beams and radiation through foils or differentially pumped sections. A novel apparatus, which utilized a short plasma arc, was successfully used to provide a vacuum-atmosphere interface as an alternative to differential pumping. Successful transmission of charged particle beams from a vacuum through the plasma to atmosphere was accomplished. Included in the article are a theoretical framework, experimental results, and possible applications for this novel interface.

© 1998 American Institute of Physics. [S1070-664X(98)91405-7]

I. INTRODUCTION

For transmission of high energy synchrotron radiation thin beryllium windows are used (or SiN in a few cases). Attenuation and spatial structure nonuniformities which attend the use of these conventional windows represent a significant problem for various applications in synchrotron radiation research. Most of the problems are the result of window heating and degradation of the radiation.

Electron beam welding (in a vacuum) has many well-known advantages over other welding techniques,¹ among which are: very high depth-to-width ratio of the weldments, very high energy efficiency, low distortions, and the ability to weld reasonably square butt joints without filler metal addition. Due to electron beam degradation in differentially pumped sections, nonvacuum electron beam welding does not possess all these advantages. Consequently, the vast majority of electron beam welding is performed under vacuum. Some of the shortcomings of vacuum welding are low production rates and limit on the size of assemblies to be welded (set by the welder vacuum system).

Widely used technologies, such as material modifications by ion implantation, dry etching, and micro-fabrication, are all performed in a vacuum, since ion beams at energies used in these applications are completely attenuated by foils and by long differentially pumped sections.

Electron beam melting for manufacturing alloys is performed at a pressure of about 10^{-2} Torr. A major drawback of operating at this pressure range is the loss of elements with low vapor pressure. Consequently, it is desirable to raise the operating pressure to a higher level.

To rectify the shortcomings of present day vacuum-atmosphere interface, differentially pumped chambers and

orifices, or thin walls, might be replaced by a short high pressure arc, which interfaces between the vacuum chamber and atmosphere and has the additional advantage of focusing charged particle beams. A novel apparatus,² which utilized such a plasma arc, was successfully used to maintain a pressure of 7.6×10^{-6} Torr in a vacuum chamber with a 2.36 mm aperture to atmosphere. Successful transmission of charged particle beams from a vacuum through the plasma to atmosphere was also accomplished.² In addition to sustaining a vacuum-atmosphere interface, the plasma has a very strong lensing effect on charged particles. The plasma current generates an azimuthal magnetic field, which exerts a radial Lorentz force on charged particles moving parallel to the current channel. With proper orientation of the current direction, the Lorentz force is radially inward. This feature can be used to focus charged particle beams to a very small spot size, and to overcome beam dispersion due to scattering by atmospheric atoms and molecules.

Plasma windows show promise as an alternative to traditional light source windows for the separation of the experimental environment from the storage ring vacuum. Inherently, such a plasma window is transparent to a wide range of the electromagnetic spectrum, from the ultraviolet out into the hard x-ray regime, and is impervious to thermal damage.

II. THEORY OF OPERATION

Plasmas can be used for vacuum separation, interface with atmosphere, and as lenses. Described below are three effects that enable that a plasma to provide a rather effective vacuum separation, and hence act as a window. Following that, the physics elements of plasma window operation and of the transmission of radiation and particle beams are discussed.

*Paper oTha12-6 Bull. Am. Phys. Soc. 42, 2006 (1997).

[†]Invited speaker.

^{a)}Electronic mail: hershcovitch@bnldag.bnl.gov

A. Ideal gas pressure effect

A most important effect is due to pressure equalization, whether it is between a discharge and atmosphere, or between a gas channel and atmosphere. Pressure is given by:

$$p = nkT, \tag{1}$$

where n is the gas or the plasma density, k is the Boltzmann constant, and T is the temperature of the gas or the plasma. In some atmospheric arcs, e.g., like that used to test this effect experimentally, the axial plasma and gas temperature can be as high as 15 000 K,³⁻⁵ with an average temperature as high as 12 000 K. Based on Eq. (1), to match atmospheric pressure at a room temperature of about 300 K, the arc plasma and gas density needs to be 1/40 of the room-temperature gas density. Therefore, an equilibrium can be reached with the vacuum chamber pressure lower by a factor of 40 (since the chamber walls are close to room temperature).

Higher temperatures were also reached³⁻⁵ in these arcs. But, due to a 50 A, limit of the arc power supply, peak parameters of the arc used as a plasma window were probably as follows: temperature 15 000 K, plasma density $1.5 \times 10^{17} \text{ cm}^{-3}$, neutral density 10^{18} cm^{-3} (peak densities concentrate in about 1 cm and fall off sharply in the rest of arc). The reason for the uncertainty is that those measurements were performed³⁻⁵ for different operating parameters (from this work): two extreme gas flows (stagnation or very high gas flow), high pressure gas feed (at least three atmospheres), and arc currents in the range of 40–200 A. Voltage drop across the arc (@ 50 A) was gas dependent: 85 V for argon, 135 V for helium, and 100 V in atmospheric air.

B. Dynamic viscosity effect

Viscosity increases with temperature. Consequently, reduction in gas flow through a hot plasma-filled channel, as compared to a room temperature gas-filled channel, is expected. Air flow, at atmospheric pressure, through a straight smooth tube of circular cross section with a very small diameter is laminar, hence, the Poiseuille equation⁶ for the gas flow rate Q applies:

$$Q = \frac{\pi d^2}{16\eta\ell} p_a(p_1 - p_2), \tag{2}$$

where d and ℓ are the tube radius and length, η is the gas viscosity, and p_a is the arithmetic mean of p_1 and p_2 . Since the viscosity of air increases with temperature,⁷ it is clear from Eq. (2) that air throughput decreases.

Some of the assumptions used to derive Eq. (2) are no longer valid once a discharge is initiated, since the flow becomes compressible and nonisothermal.⁵ Therefore, a thorough analysis of gas and plasma flow requires the solution of coupled transport equations for ions and electrons, as well as the Navier–Stokes equation for the gas. For electrons and ions, the relevant transport equations are the continuity and momentum transfer equations⁸

$$\frac{D}{Dt} n_{e,i} + n_{e,i} \nabla \cdot \underline{V}_{e,i} = 0, \tag{3}$$

$$m_{e,i} n_{e,i} \frac{D}{Dt} \underline{V}_{e,i} = -\nabla p_{e,i} - \nabla \cdot \underline{P}_{e,i} + q_{e,i} n_{e,i} [\underline{E} + \underline{V}_{e,i} \times \underline{B}] + \underline{R}_{e,i}, \tag{4}$$

where m is the particle mass and q its charge. \underline{R} is the species total momentum transfer, p its partial pressure, and \underline{P} is the stress tensor; and $D/Dt = \partial/\partial t + \underline{V} \cdot \nabla$. The Navier–Stokes equation is basically the momentum equation [Eq. (4)] without the electric and magnetic field terms. It is usually written in a notation in which $nm = \rho$, $\underline{R} = \underline{f}$, and with a partially expanded stress tensor. To close this set of equations, more equations (e.g., energy transport) must be added and some assumptions must be made in order to truncate the equations. Solving this set of equations is beyond the scope of this paper. Nevertheless, it can be shown qualitatively, from this set of equations, that thermal effects play a significant role in reducing gas throughput through a plasma-filled channel. The stress tensor \underline{P} is directly proportional to the viscosity η , which in turn has a very strong temperature dependence.⁷⁻⁹ For ions and electrons⁸

$$\eta_i = 2 \times 10^5 \mu^{1/2} \frac{k}{\lambda_i} T_i^{5/2}, \text{ and } \eta_e = 2.5 \times 10^7 \frac{k}{\lambda_e} T_e^{5/2}, \tag{5}$$

where λ is the Coulomb logarithm and μ is the ion mass expressed in proton mass units. For gases, the simplest expression for viscosity is^{7,9}

$$\eta = aT^x, \tag{6}$$

where a and x are constant characteristics of each gas. For air, e.g., at about 1000 °F, x is somewhat larger than 1. Consequently, the gas flow through a plasma-filled channel should be greatly reduced, due to the strong enhancement in viscosity at high temperatures.

C. Ionization effect

A smaller contribution is expected from ionization of molecules and atoms by plasma particles. A quick comparison between the ionization time [given by $(n_e \sigma v)^{-1}$, where σ is the effective ionization cross section] for an atom or a molecule entering a 6 cm long, 2 mm diameter channel through which a 50 A, 100 V electron current flows, and the atom or molecule transit time reveals that the ionization time is of the order of 0.1 μs , while the transit time is of the order of 10 s of μs . Thus the ionization probability is extremely high. This effect is very important in cases where gas flows are low. At steady state high flow rates, the plasma density will build up quickly to reach an equilibrium when plasma build-up is matched by recombinations and other neutralizing effects. This plasma accumulation creates the ‘‘plug’’ that was analyzed in the previous paragraphs. Additionally, this effect can make a useful contribution to some applications (e.g., electron beam welding) by preventing metal chips and vapor from backstreaming into an electron beam column.

D. Plasma lens

In a beam of charged particles, propagating through a field-free region, there are two forces acting on the particles: space charge forces trying to “blow” the beam up, and a magnetic force pinching the beam¹⁰ (due to the magnetic field generated by the beam current). This magnetic force is a consequence of the Lorentz force, F , given by:

$$F = qV \times B, \quad (7)$$

where q is the particle charge, V its velocity, and B is the magnetic field. When a beam enters a plasma, space charge forces are neutralized, hence, beam focusing results from the magnetic field. If the plasma carries a current, the resulting magnetic field must be added to Eq. (7). In all cases of interest to this subject matter, currents generated in the arcs far exceed the beam currents, so beam self-focusing is negligible.

E. Electron beam propagation

Next, calculations are made to examine propagation of an electron beam through a current-carrying plasma window. A fractional ionization of 15% is considered.¹¹ Scattering of beam electrons by various particles leads to beam expansion, since scattering acts as a source of beam transverse energy, T_{\perp} . For gas scattering, growth is given by¹²

$$\frac{dT_{\perp}}{dz} = \frac{4\pi e^4 n Z(Z+1)}{\beta^2 \gamma m c^2} \ln \left[\frac{192 \beta \gamma}{Z^{1/3}} \right], \quad (8)$$

where n is the atomic density number, Z is the atomic number, m is the electron mass, c is the speed of light, β and γ are the well-known relativistic quantities. The electron beam is propagating in the z direction. The elementary charge is e .

Equation (8) together with the beam envelope equation¹³ can be used to rigorously calculate the electron beam dynamics through the plasma window. The beam envelope equation,

$$\frac{d^2 R}{dz^2} + \kappa R - \frac{K}{R} - \frac{\epsilon_{\perp}^2}{R^3} = 0, \quad (9)$$

describes growth in beam radius R as a function of propagation distance z . Beam focusing function is described by κ , ϵ_{\perp} is the transverse emittance, and the generalized perveance $K = 2I_b / (\beta \gamma)^3 1.7 \times 10^4$ (which describes space charge driven radial growth in a beam with a current I_b). However, inside the plasma window the space charge term is negligible. Growth in transverse beam energy T_{\perp} [as given by Eq. (8)] increases emittance¹⁴ as $\epsilon_{\perp} = 2R(kT_{\perp}/mc^2)^{0.5}$. Substituting this complex term of emittance into Eq. (9) yields an expression for radial beam growth due to gas scattering [last term in Eq. (9)]. Computing the focusing function κ [for substitution into Eq. (9)] requires knowledge of the radial current profile of the plasma channel. Evaluating such an expression must be done numerically even for the simplest cases. Hence, solving Eq. (9) rigorously requires a numerical solution which is beyond the scope of this work. Although this problem is as complex as that of relativistic electron beams propagating through atmosphere,¹⁵ simplified calcula-

tions can provide insights on the lensing effects of such a current-carrying plasma channel. In Ref. 2, gain in transverse beam energy was treated as an effective electron transverse acceleration, which was balanced by a radially inward Lorentz acceleration. The Lorentz force was calculated from Eq. (7), and B_{θ} the azimuthal magnetic field generated by the plasma current I , was calculated from Ampere's Law

$$B_{\theta} = \frac{\mu_0 I}{2\pi R}. \quad (10)$$

For a helium plasma channel of 1 mm radius, and an electron beam energy of 175 keV with a 1° divergence, arc current $I = 29$ Amperes was needed to prevent beam dispersion due to scattering. Next, two additional estimates, of the plasma channel arc current needed to compensate for electron beam dispersive effects, are presented. Capturing and focusing of charged particles in current-carrying plasma channels (lens) has been used in high energy physics¹⁶ and ion fusion¹⁷ research. The current needed in a channel to capture a charged particle entering on axis at an angle θ with an energy E is

$$I_{\text{ch}} = (2^{3/2} \pi / \mu_0) (mE/Ze)^{1/2} \theta^2. \quad (11)$$

To capture an electron beam with the above parameters, I_{ch} of only 2 A is needed. If however, the electrons are scattered and heated [Eq. (8) yields $T_{\perp} = 1.36$ keV in about 1 cm; peak plasma density falls sharply after about 1 cm^{-3-5}], θ can increase to about 5.2° and the needed $I_{\text{ch}} \approx 55$ A.

Another approach is to equate the pressure of the heated electron beam to the “pinching force” exerted by the azimuthal magnetic field. In effect, treat the electron beam as a single fluid in Eq. (4) and consider the radial component under this “pinch equilibrium” such that

$$\nabla_r p = J_z \times B_{\theta}, \quad (12)$$

where B_{θ} is given in Eq. (10) and J_z is the electron beam current density. But, $\nabla_r \sim 1/R$, $J = env$, p and B_{θ} are given in Eqs. (1) and (10), respectively. Solving Eq. (12) for I yields, $I = 2\pi kT_{\perp} / e\mu_0 \beta c$, and T_{\perp} can be solved from Eq. (8). For beam heating resulting in $T_{\perp} \approx 1.36$ keV, the needed $I = 25$ A. It is clear from these estimates that a plasma window carrying a current of 25–50 A, can compensate for dispersive effects, and larger currents will result in electron beam focusing.

Collisions do not only scatter the beam, but also extract energy¹²

$$\frac{dE}{dz} = \frac{4\pi e^4 n Z}{m c^2 \beta^2} \left[\ln \left(\frac{2m c^2 \beta^2 \gamma^2}{W} \right) - \beta^2 \right], \quad (13)$$

where W is a typical molecular excitation energy that is of the order of about 10 eV. For the above beam and plasma parameters, Eq. (13) yields $dE/dz \approx 300$ eV/cm, which represents a relatively small energy loss.

In the preceding analysis, dispersive effects and attenuation by ions and electrons were neglected. To a first approximation, this assumption is correct. Examining expressions for slowing down and transverse diffusion rates for 175 keV electrons streaming through such a helium plasma, in-

indicates that the fastest relaxation rate is the transverse diffusion due to collisions with ions and electrons. An expression from Ref. 18, for this relaxation, yields a transverse temperature growth rate of $dT_{\perp}/dz = 14 \text{ eV/cm}$. By comparison, Eq. (8) yields $dT_{\perp}/dz = 1.356 \text{ keV/cm}$.

F. Ion beam propagation

Although the physics of the lensing effects for ions is similar to that of electrons, the magnitude of this effect on ions is much lower due to their lower velocity and larger mass. Moreover, passage of ions through gas and plasma is dominated by slowing down interactions rather than transverse diffusion.

For many applications, e.g., microfabrication, ion beams with very small spot sizes (as low as 50 nm^{19}) are used. Therefore, the ion beam passes through the channel axis, i.e., through the hottest part of the plasma and gas where the temperature is $15\,000 \text{ K}$. Thus based on Eq. (1), the helium gas density at the interface with atmosphere is $n = 10^{18} \text{ cm}^{-3}$. And, for a 15% fractional ionization, the plasma density is $1.5 \times 10^{17} \text{ cm}^{-3}$.

Examining plasma effects,¹⁸ the fastest relaxation rate is the slowing down of ions by plasma electrons (dynamic friction) given by¹⁸

$$\nu_s = 1.7 \times 10^{-4} n \lambda Z^2 \mu^{1/2} E^{-3/2}. \quad (14)$$

And, the forward velocity slowing down rate is $dV_z/dt = -\nu V_z$.

For a 400 keV Ga^+ beam, Eq. (14) yields $\nu_s = 1.3 \times 10^7 \text{ s}^{-1}$, and, since the ion velocity is $1 \times 10^8 \text{ cm/s}$ at this energy, the energy attenuation rate is about 50 keV/cm ; hence at the channel exit, the beam energy is expected to be of the order of 100 keV .

Ion attenuation by gas is also dominated by energy loss. The total energy loss can be calculated from the Bethe-Block equation^{20,21}

$$\frac{dE}{dz} = \frac{4\pi e^4 Z^2}{mV^2} nZ' \left[\ln \frac{2mV^2}{W} - (1 - \beta^2) - \beta^2 \right], \quad (15)$$

where Z' is the atomic number of the gas atoms and W is an empirical constant known as the geometric-mean ionization and excitation potential (of the order of 100 eV). For a 400 keV Ga^+ beam, Eq. (15) yields an energy loss rate that is about 9 keV/cm .

G. Transmission of synchrotron radiation

In absence of resonances, plasmas are transparent to electromagnetic radiation whose frequency exceed the plasma frequency ω_p . At a plasma density of $1.5 \times 10^{17} \text{ cm}^{-3}$, $\omega_p = 3.5 \times 10^{12} \text{ Hz}$ and a corresponding wavelength λ of about $86 \mu\text{m}$. Radiation, with a wavelength shorter than $86 \mu\text{m}$, is not affect by collective plasma processes. Cross sections for interaction of radiation, in the electromagnetic spectrum from ultraviolet out into the hard x-ray regime, with individual particles is usually minuscule, e.g., for Thompson scattering $\sigma = 2/3 \text{ barn}$. For photon energies of a few 10^3 's of eV, some photo-absorption and photo-

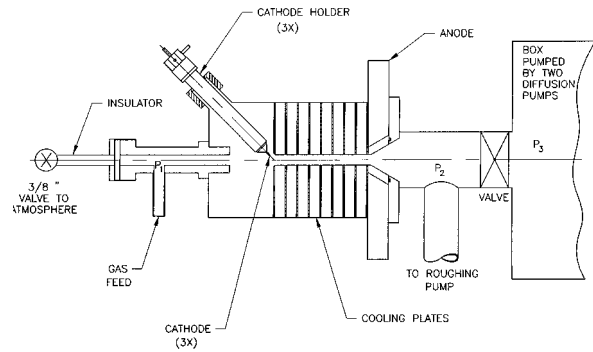


FIG. 1. Schematic (not to scale) of the setup for the vacuum-atmosphere interface experiment. The cascade arc is enlarged to show details of its main components: cathodes and cooling plates. P_2 is measured in a 4 in. pipe, while P_3 is measured in a box whose dimensions are 2 ft \times 2.5 ft \times 4 ft.

ionization cross sections can reach the 10^{-19} – 10^{-18} cm^2 level. However, this type of absorption is species dependent, and it affects only discrete lines.

Basically, plasma windows are expected to have negligible interaction with electromagnetic radiation in the spectra generated in synchrotron light sources. Furthermore, the target thickness of a plasma window $nl \approx 1.5 \times 10^{17} \text{ cm}^{-2}$ is about 4 orders of magnitude lower than that of a conventional $200 \mu\text{m}$ beryllium window with $nl \approx 2.5 \times 10^{21} \text{ cm}^{-2}$.

Radiation emitted by the plasma, although at energies significantly lower than that of synchrotron radiation, can be fairly intense and affect very sensitive instruments. For an electron temperature of about 10 eV (upper limit), the bremsstrahlung radiation (which far exceeds all other emissions in the visible to UV range) $P = 1.69 \times 10^{-32} n T^{0.5} \sum Z^2 n(z)$ is about 1.2 kW/cm^3 .

III. EXPERIMENTAL RESULTS

A number of experiments were performed with an arc driven plasma to examine its potential for a plasma window. These studies were a series of differential pumping experiments (with and without venturi gas feed), an electron beam propagation test, a series of electro-magnetic interference (EMI) experiments, and a test in which the plasma separated a high pressure chamber and atmosphere. Experimental details are presented in the following sub-sections.

A. Differential pumping experiments with conventional gas feed

Figure 1 shows the experimental setup that was used to determine the effectiveness of using an arc as a vacuum-atmosphere interface. The arc is a wall-stabilized type cascade arc discharge^{3–5} that was purchased from D. Schram's group at Eindhoven University of Technology. In this setup, the cathodes were at the atmospheric end of a channel that was 2.36 mm in diameter (0.093 in.) and 6 cm long. At the

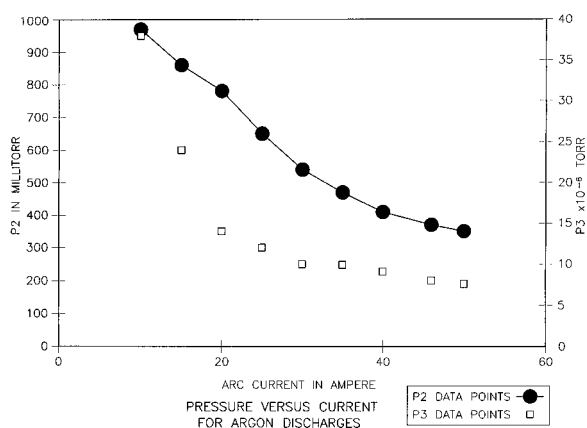


FIG. 2. With $P_1 = 760$ Torr, P_2 and P_3 are displayed as a function of the arc current in argon discharges.

chamber end a valve was mounted on an insulator. This valve was opened to atmosphere after discharge initiation and a subsequent elevation of P_1 to atmospheric pressure. The opposite end of the channel was opened to a 4 in. pipe, pumped by a mechanical pump, on which the cascade arc was mounted. This pipe was connected to a box (partially shown in Fig. 1) through a valve. The maximum arc current was 50 A in noble gases. Prolonged operation in atmospheric air resulted in erosion, by oxygen, of the copper cooling plates. Pressure at P_1 and P_2 was measured with Granville-Phillips thermocouple gauges, and in addition, P_1 was also measured with a HEISH absolute mechanical pressure gauge that utilizes a Bourdon tube. A Perkin-Elmer ULTEX ionization gauge was used to measure P_3 .

Using only differential pumping and opening the valve to atmosphere with no discharge, $P_1 = 760$ Torr and $P_2 = 80$ Torr was measured. After the discharge was initiated in argon, P_1 was set slightly above atmosphere, and the valve was opened. As the arc current was raised from 10 A to 50 A, the pressure at P_2 decreased with increasing arc current, reaching 350 mTorr at 50 A. This represents a reduction by a factor of 228.6 over differential pumping.

Figure 2 shows the pressures P_2 and P_3 as a function of the arc current for discharge in argon, where P_1 was at 760 Torr. Next, the gas feed was switched to helium, and the same measurements were repeated with helium as the discharge gas. The results were similar, although the pressures at P_2 and P_3 were higher by a factor of about 2.8 for the same arc currents.

Qualitatively, the results displayed in Fig. 2 are consistent with the theoretical arguments introduced in the previous section. The plasma and gas temperatures, as well as ionization fraction, are known to increase with increasing arc current.³⁻⁵ Therefore, the plasma and gas viscosities are expected to rise with the increase in arc current, while the gas density is expected to decrease with increasing arc current. Consequently, P_2 and P_3 , as expected, decrease with increasing arc current. Quantitatively, based on the discussion in Sec. II A, the effect based on Eq. (1) can account for a factor of 40 in pressure reduction at P_2 . The extra factor of

5.7 reduction in P_2 is most likely due to increase in viscosity.

B. Differential pumping experiments with venturi gas feed

In a new experimental set-up, the gas feed of Fig. 1 was replaced by a venturi. The vacuum box was eliminated, and the valve was replaced by a viewing port. A convectron gauge is used to measure the pressure in the 4 in. pipe vacuum. The venturi is a novel feature incorporated in this plasma window.

Gas supply for this window is fed through the venturi. The rationale for using the venturi is to utilize the gas to enhance the differential pumping. Experimentally, there was a further enhancement in the plasma window performance by another factor of 3, i.e., the difference in the pressure in the 4 in. pipe (plasma window on versus plasma window off) was a factor of 600. Thus the enhancement over differential pumping was a factor of 600 with the venturi (compared to 228.6 without the venturi). Additionally, with the venturi, there was a 25% reduction in power consumed by the plasma window arc. Obviously much of the enhancement can be attributed to pressure reduction at the cathodes. It is not clear whether there are other contributing factors (like higher temperature or enhanced viscosity).

Further reduction of about 16% in pressure was observed when a solenoid generating a peak magnetic field of 3.1 kG was placed at the vacuum end of the plasma window. The coil functioned as a magnetic mirror, preventing some charged particles from entering the 4 in. pipe. Although the improvement was small, the results strongly suggest that plasma window performance can be further enhanced with magnetic fields.

Finally, an experiment performed with the arc reversed (gas feed and flow were reversed, the anode was on the atmosphere side), as shown in Fig. 3, yielded identical results. It indicates that thermal effects like gas pressure and viscosity are dominant, while inter-species momentum transfer, gas and plasma flows can be neglected (to first order). In that set-up, the plasma channel was only 3 cm long (instead of 6 cm), which strongly suggests that the plasma pressure gradient is rather steep.

C. Electron beam transmission experiment

The Fig. 1 set-up with some slight modifications was used for a quick test of electron beam propagation through helium cascade arc discharges with P_1 set at 760 Torr. The anode of the cascade arc discharge was mounted on a PTR #727 electron beam welder. Copper and steel plates were mounted 1 centimeter away from the cathodes (and channel exit). The distance from the electron beam welder exit to the first plate was 12 cm. Thus the electron beam had to travel through 5 cm of fairly good vacuum, 6 cm of plasma (in the channel), and 1 cm of atmospheric pressure helium gas. The electron beam energy used in the experiment was 175 keV with a current level of up to 20 mA.

Detailed quantitative measurements of electron beam transmission could not be done without major modifications

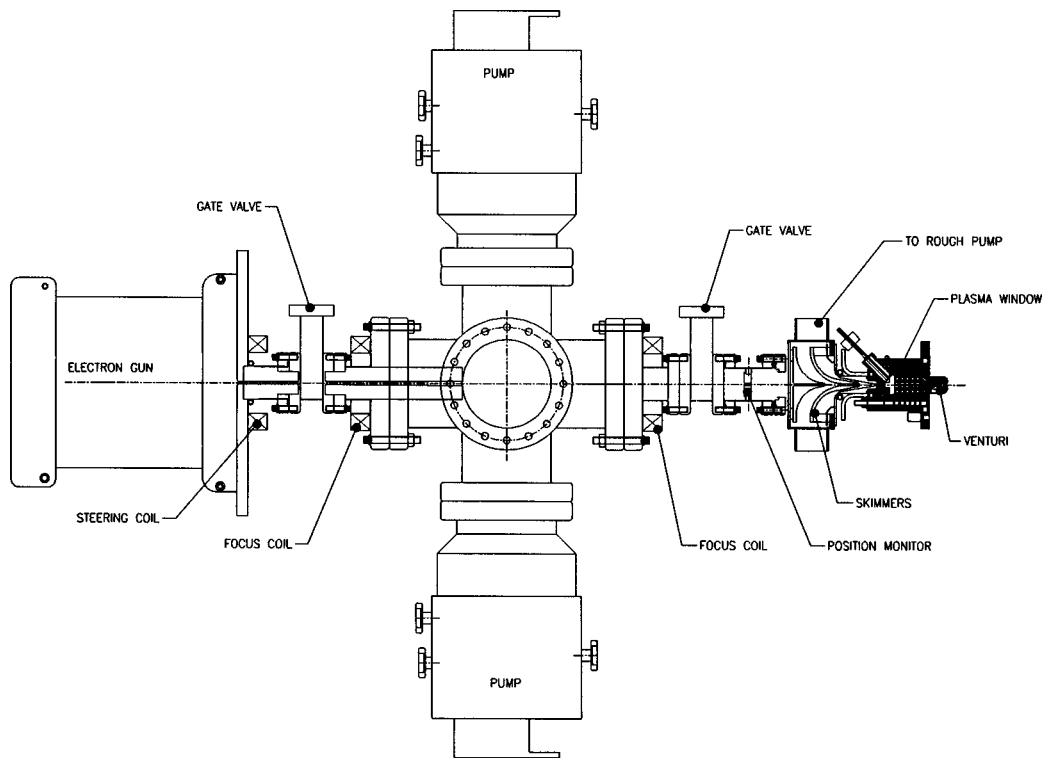


FIG. 3. Conceptual design of a nonvacuum electron beam welder (courtesy of Litton Electron Devices).

of both the electron beam welder and the cascade arc discharge. At the welder exit, the electron beam had a diameter of 0.5 mm and half-angle divergence of 1° . Consequently, at the arc entrance, its diameter of 2.24 mm is almost as large as the arc channel. In addition to beam interception by the cooling plates, a Faraday cup could not be used without a complete redesign of the arc cathode housing geometry.

Successful electron beam propagation was observed, qualitatively from the melting of the copper plates, and from holes drilled through the steel plates by the electron beam. The propagation was facilitated by the arc discharge since no beam propagation was observed with the arc off.

There was no beam blow up, since the size of the holes drilled through the steel plates were about 2 mm, i.e., smaller than the channel diameter of 2.36 mm and the 4.5 mm diameter the electron beam would have been after 12 cm due to the 1° (half-angle) divergence.

D. Compatibility tests for transmission of electromagnetic radiation

Before proceeding with plasma window development for light sources, it was crucial to ensure that plasma windows do not generate electromagnetic interference, which would adversely affect experiments. Therefore, a series of electromagnetic interference tests had to be conducted.

A series of electro-magnetic interference (EMI) experiments revealed that rf emission from the Fig. 1 plasma window is negligible. In these experiments, no EMI or electromagnetic noise was detected on: a radio, a "Walkman," and a computer (PC) operating adjacent to the plasma window. Quantitatively, an EMI probe in the range of 30–300 MHz

detected rf noise of up to 0.7 mW/cm^2 on the arc power supply, and up to 0.9 mW/cm^2 on the arc circuit. However, on the plasma window itself, only 0.05 mW/cm^2 could be measured. The reason may be due to the fact that plasma frequency is so high that only electromagnetic radiation with a frequency higher than IR can escape.

Finally, the "acid" test for rf noise was passed. In this test, the most noise sensitive electronics at the National Synchrotron Light Source at Brookhaven National Laboratory functioned well while the plasma window operated. These were the proportional counter electronics belonging to Kirz and Feser of SUNY Stony Brook.

Since gas rushing out from a venturi may be objectional to some users, experiments were performed to reduce axial gas flow with a funnel and by deflection. A combination of the two yielded a factor of 30 reduction in axial pressure.

Due to interest in using plasma windows in powerful gas lasers, the plasma window was successfully used to separate a high pressure (68 psi) chamber and atmosphere. A 5 mW He-Ne laser beam (with a 543 nm wavelength) was passed from that chamber through the plasma window to atmosphere.

IV. DISCUSSION

Vacuum-atmosphere interface was successfully established with helium or argon cascade arc discharge plasmas. A 175 keV electron beam was transmitted from a vacuum through a helium plasma channel to strike targets at atmospheric pressure located 1 cm away from the channel exit.

Calculations carried out in this paper indicated that the arc current of such a plasma channel can focus electrons or

ions, to compensate for gas scattering and initial geometric beam divergence. For electron beams used in welding or melting, estimates based on various physical effects indicate focusing feasibility. Due to the large variety of ions and the wide range of ion energies used in material modifications, detailed analysis of ion beam attenuation and focusing is needed for each application. Nevertheless, since the principle of this type of focusing had been demonstrated,^{16,17} and since data²² indicates a reasonable range of ions in air, nonvacuum ion material modification seems feasible, with such a vacuum-atmosphere interface.

Based on obtained results, utilization of plasma windows in electron beam welding seems feasible. Figure 3 is a schematic of an experimental electron beam welder. Among some of the benefits of using this type of vacuum-atmosphere interface are the increase in production rate, and the potential of performing electron beam welding and various types of ion material modifications on large work pieces and in previously inaccessible places. Cooling plates can be miniaturized to provide for a long narrow discharge channel, to reach previously inaccessible places.

Establishment of a vacuum-atmosphere interface with out any intrusive solid structures, and without EMI, strongly suggests feasibility to light source applications. Inherently, such a plasma window is transparent to a wide range of the electromagnetic spectrum, from the ultraviolet out into the hard x-ray regime. The development of the plasma window for synchrotron radiation applications could have an important impact on light source facilities around the world. Attenuation and spatial structure which attend the use of conventional window materials (e.g., beryllium or SiN) represent a significant problem for various applications in synchrotron radiation research. These include microspectroscopies and some types of correlation spectroscopies. Plasma windows show promise as an alternative to traditional windows for the separation of the experimental environment from the storage ring vacuum. They would possess none of the structure that has hindered the development of speckle experiments at low energies (a few keV), and would be impervious to thermal damage. In addition, the plasma may contain noble gases, which would provide efficient high-order rejection for UV experiments, such as threshold photo-ionization spectroscopies.

High pressure-atmosphere separation capability points to possible utilization of plasma windows in intense gas lasers and for the CO₂ laser amplifier, while vacua separation can render plasma windows useful in electron beam melting and in various scientific applications requiring internal targets like an electron beam plasma accelerator.

To further enhance window performance, skimmers like those shown in Fig. 3 can be added, as well as magnetic confinement. Mutually perpendicular electric and magnetic fields can be added in such a way that the resultant drifts guide escaping ions back into the window (based on plasma

thruster principle). Plasma thrusters can potentially “seal” plasma windows, or at least significantly reduce (or even eliminate) the number of supersonic particles resulting in conventional differentially pumped systems (which prevented their use in light sources²³).

ACKNOWLEDGMENTS

Many thanks to Daan Schram and his group at Eindhoven (especially Ries van de Sande) for help with the cascade arc device. For some experiments technical support was provided by W. Tramm, W. Hensel, G. LaFlamme, E. Smith, J. Kennedy, D. Deb, N. Samaniego, and J. Poff. Special thanks to D. Langiulli and D. Rosenbaum for support of some projects. Contribution from students P. Kollman, A. Jeffers, and C. Castle was invaluable in setting up experiments and in data collection. Many stimulating discussions with and valuable advice from Erik Johnson, Pete Stefan, and Dick True is gratefully acknowledged. Work was performed under the auspices of the U.S. Department of Energy.

¹Y. Arata, *Plasma, Electron and Laser Beam Technology* (American Society of Metals, Metals Park, OH, 1986); N. Taniguchi, *Energy-Beam Processing of Materials* (Oxford Science Publications, Clarendon, Oxford, 1989).

²A. Hershcovitch, *J. Appl. Phys.* **78**, 5283 (1995).

³C. J. Timmermans, R. J. Rosado, and D. C. Schram, *Z. Naturforsch. A* **40**, 81 (1985).

⁴G. M. W. Kroesen, D. C. Schram, and J. C. M. de Haas, *Plasma Chem. Plasma Process.* **10**, 531 (1990).

⁵J. J. Beulens, D. Milojevic, D. C. Schram, and P. M. Vallinga, *Phys. Fluids B* **3**, 2548 (1991).

⁶L. D. Landau and E. M. Lifshitz, *Fluid Mechanics* (Addison-Wesley, Reading, MA, 1959).

⁷R. L. Daugherty and A. C. Ingersoll, *Fluid Mechanics* (McGraw-Hill, New York, 1954).

⁸S. I. Braginskii, *Reviews of Plasma Physics*, Vol. 1 (Consultants Bureau, New York, 1965), pp. 205–311.

⁹S. Chapman and T. G. Cowling, *The Mathematical Theory of Non-Uniform Gases* (The University Press, Cambridge, England, 1939).

¹⁰W. H. Bennett, *Phys. Rev.* **45**, 890 (1934).

¹¹D. C. Schram, private communication, 1993; although this fractional ionization can be as high as 70% on axis.

¹²Expressions derived from H. A. Bethe's work, e.g., J. D. Jackson, *Classical Electrodynamics*, 2nd ed. (Wiley, New York, 1975).

¹³I. M. Kapchinskij and V. V. Vladimirovskij, *Proceedings of the International Conference on High Energy Accelerators*, Geneva, 1959 (Lern, Geneva, 1959), pp. 274–188.

¹⁴J. D. Lawson, *The Physics of Charged Particle Beams* (Oxford University Press, Oxford, 1977), p. 175.

¹⁵R. F. Fernsel, R. F. Hubbard, and M. Lampe, *J. Appl. Phys.* **75**, 3278 (1994).

¹⁶M. Giesch, B. Kuiper, B. Langeseth, S. Van Der Meer, D. Neet, G. Plass, G. Pluym, and B. De Raad, *NIM* **20**, 58 (1963).

¹⁷C. L. Olson, *J. Fusion Energy* **1**, 309 (1982).

¹⁸B. A. Trubnikov, *Reviews of Plasma Physics*, Vol. 1 (Consultants Bureau, New York, 1965), pp. 105–204.

¹⁹P. D. Prewett, *Rev. Sci. Instrum.* **63**, 2364 (1992).

²⁰H. A. Bethe, *Ann. Phys. (Leipzig)* **5**, 325 (1930).

²¹H. A. Bethe, *Z. Phys.* **76**, 293 (1932).

²²R. D. Evans, *The Atomic Nucleus* (McGraw-Hill Co., New York, 1970); see e.g., data in Chap. 22 on range of α particles and fission fragments in air; J. Boggild, K. Bronstrom, and T. Lauritsen, *Phys. Rev.* **59**, 275 (1941).

²³P. Stefan (private communication, 1997).